JOURNAL OF GUIDANCE, CONTROL, AND DYNAMICS
Vol. 16, No. 6, November–December 1993

H^∞ Robust Control Design for Linear Feedback Systems

Jiann-Shiou Yang
University of Minnesota, Duluth, Minnesota 55812

This paper deals with the problem of designing, for a linear time-invariant multivariable plant, a feedback controller that minimizes the H^∞ norm of a quadratic combination of the sensitivity and complementary sensitivity functions. With the parameterization of the controller and quadratic cost, a design procedure based on a gain equalization test for computing the optimal controller is described in detail. A design algorithm, which is implementable in computers, is presented. The pitch-axis controller design for a digitized version of the Grumman F-14 aircraft is given. The performance robustness under the external disturbances and large aircraft parameter variations are shown to demonstrate the effectiveness of this approach.

Introduction

IN the past several decades, the problem of multivariable control system design has been studied intensively by many researchers. Feedback has been used in control system engineering as a means to satisfy design requirements such as system stabilization, reduction of system response to external disturbances, realization of specified transient response and/or frequency response characteristics, and improvement of a system's robustness against variations in open-loop dynamics. A standard H^∞ control problem is to synthesize a feedback controller for a linear time-invariant plant that internally stabilizes the closed-loop system and satisfies an H^∞-norm bound on a specified closed-loop transfer function. Initiated by Zames,[1] the H^∞ approach itself has undergone considerable development and elaboration since.[2,3]

It is well known that, for robust control system design, minimizing only the sensitivity or only the complementary sensitivity function suffers serious drawbacks. A tradeoff should be considered in the design process. Various mixed H^∞ sensitivity methods have been reported in the literature.[4,5] In Ref. 6, Kwakernaak considered a mixed sensitivity minimization using a polynomial approach. His solution involves solving a set of nonlinear equations and has numerically encountered some difficulties with convergence. In this paper, an H^∞ controller design based on the minimization of a quadratic combination of the sensitivity and complementary sensitivity matrices is posed. The criterion we choose is similar to that of Kwakernaak,[6] but the approach is different. We use the technique of designing broadband circuits, particularly gain equalization problems, to optimize the robustness of the control systems. Our approach is divided into two steps: 1) determine the optimum value that the parameterized criterion can reach using a gain equalization test[7,8]; and 2) solve a rational matrix equation for the optimal controller. We first give the problem formulation and show some properties about the parameterized criterion. A design procedure using a gain equalization test is then presented to find the optimal controller. The controller design algorithm, which is implementable in computers, is also shown. We then apply the design method to a digitized version of the Grumman F-14 pitch axis control problem to demonstrate the effectiveness of this approach. This is followed by concluding remarks.

The notation used in this paper is fairly standard. Let I_n be an $n \times n$ identity matrix. A real-rational matrix $G(s)$ is proper if it does not have a pole at infinity, strictly proper if $G(\infty) = 0$, and stable if it is analytic in the closed right half-plane. A real-rational matrix $G(s)$ is para-Hermitian if $G^*(s) = G(s)$, where $G^*(s) = G^T(-s)$, and T means the transpose. For a square matrix M, $\det(M)$ and $\lambda_{\max}(M)$ are the determinant and the maximum eigenvalue of M, respectively. The symbol $R(s)^{p\times q}$ denotes the set of all $p \times q$ real-rational matrices in s. Let RH^∞ be the set of all stable, proper, real-rational functions, and RL^∞ denote the set of proper, real-rational functions with no poles on the $j\omega$ axis. The symbols $(RL^\infty)^{p\times q}$ and $(RH^\infty)^{p\times q}$ are the sets of $p \times q$ matrices with elements in RL^∞ and RH^∞, respectively, and $M(RH^\infty)$ denotes the set of matrices whose elements belong to RH^∞. The L^∞/H^∞ norm of a stable, proper, real-rational matrix $G(s)$ is defined as $\|G\|_\infty = \sup_\omega \bar{\sigma}[G(j\omega)]$, where $\bar{\sigma}(G)$ denotes the maximum singular value of G. Let $G \in RL^\infty$; then T_G and H_G denote the Toeplitz matrix and Hankel matrix generated by G, respectively. The notation $\max(a, b)$ gives the larger value of a or b. Any real-rational matrix $G(s)$ can be uniquely partitioned as the sum of two parts, $[G(s)]_+$ and $[G(s)]_-$ with $[G(s)]_+$ strictly proper and stable and $[G(s)]_-$ the remainder of $G(s)$.

Problem Formulation

Consider a standard unity feedback control system with plant $G(s) \in R(s)^{n\times m}$ and controller $F(s) \in R(s)^{m\times n}$. Then the system sensitivity matrix $S(s)$ and complementary sensitivity matrix $T(s)$ are defined, respectively, as $S(s) = [I_n + G(s)F(s)]^{-1}$ and $T(s) = I_n - S(s)$. It is known that $S(j\omega)$ directly quantifies such feedback properties as output disturbance reduction and sensitivity to plant parameter variations. This can be achieved by requiring that $\bar{\sigma}(\tilde{W}_1 S)$ is small for all ω, where $\tilde{W}_1$ is a weighting function that is suitably chosen in relation to the plant $G(s)$ and the available information about

Jiann-Shiou Yang received the B.S. degree in control engineering from National Chiao Tung University, Hsinchu, Taiwan, in 1976, and received the M.S. and Ph.D. degrees in electrical engineering from the University of Maryland, College Park, in 1983 and 1988, respectively. He was awarded an IBM fellowship from 1985 to 1986, and from 1986 to 1988 he was a fellow at the Institute for the System Research, University of Maryland, College Park. He is an Assistant Professor of Computer Engineering at the University of Minnesota, Duluth, where he teaches control systems, digital control system design, and robotics. His research interests include robust multivariable control, system theory, and computer-aided control system design. He is a Member of AIAA.

Received Oct. 19, 1992; revision received Feb. 2, 1993; accepted for publication Feb. 4, 1993.

the frequency content of the disturbances. The function $T(j\omega)$ is directly related to the sensor noise attenuation, bandwidth limitation, and plant saturation avoidance. Limitation can be achieved by imposing a bound on $\bar{\sigma}(\bar{W}_2 T)$, where $\bar{W}_2$ is a suitable weighting function reflecting the available information about the frequency content of the sensor noise and command input. However, it is impossible to make both small at every frequency.

For realistic control design, many essential design objectives can be formulated as bounds on the weighted S and T. For the single-input single-output case, it is concluded that a balance between conflicting design objectives can be achieved by minimizing a performance criterion of the form $\sup_\omega [|\bar{W}_1(j\omega)S(j\omega)|^2 + |\bar{W}_2(j\omega)T(j\omega)|^2]$.[5] We consider the extension of this mixed criterion to the multivariable case. For the system given, consider a quadratic combination of the weighted $S(s)$ and $T(s)$, i.e., $(\bar{W}_1 S)^*(\bar{W}_1 S) + (\bar{W}_2 T)^*(\bar{W}_2 T) = S^* \bar{W}_1^* \bar{W}_1 S + T^* \bar{W}_2^* \bar{W}_2 T$. The matrices $W_1(s)$ and $W_2(s)$, defined by $W_1(s) = \bar{W}_1^*(s)\bar{W}_1(s)$ and $W_2(s) = \bar{W}_2^*(s)\bar{W}_2(s)$, are frequency-dependent weighting matrices. We want to design a controller $F(s)$ to stabilize the given plant $G(s)$ and, at the same time, to minimize

$$\text{(P)} \qquad \min_{F(s)} \|(S^* W_1 S + T^* W_2 T)(j\omega)\|_\infty$$

The choice of weights is problem specific; in general, these user-defined weights are chosen to be stable, diagonal with the diagonal elements to be minimum phase, and real rational. With diagonal weights, each one of the input and output signals can be weighted individually. Thus, the designer can easily trade off the relative importance of the weights over the same or different frequency bands. We assume that $G(s)$ is strictly proper and $\bar{W}_1(s)$, $\bar{W}_2(s) \in R(s)^{n\times n}$ are nonsingular, proper, stable, and have no poles on the $j\omega$ axis.

Lemmas 1 and 2 are easily verified and are given without proof.

Lemma 1. $W_1(s)$, $W_2(s) \in R(s)^{n\times n}$ are nonsingular, proper, para-Hermitian matrices with no poles on the $j\omega$ axis and $W_1(j\omega) \geq 0$, $W_2(j\omega) \geq 0, \forall\omega$.

Lemma 2. $W_1(s) + W_2(s) \in R(s)^{n\times n}$ is a proper, para-Hermitian matrix with no poles on the $j\omega$ axis and $(W_1 + W_2)(j\omega) \geq 0, \forall\omega$.

Lemma 3. The inverse of $(W_1 + W_2)$ exists on the $j\omega$ axis.

The proof of Lemmas 3, 5, and 6 are given in the Appendix. From Lemmas 2 and 3 and Ref. 9, we have

Lemma 4. (Spectral factorization) There exists a spectral factor $M(s)$ such that $W_1(s) + W_2(s) = M^*(s)M(s)$ where $M(s)$, $M^{-1}(s) \in (RH^\infty)^{n\times n}$, and such an $M(s)$ is unique up to left multiplication by a constant unitary matrix.

Let $\Omega(G)$ denote the set of all real-rational controllers $F(s)$ that stabilize $G(s)$. Then it is well known that[10] $\Omega(G) = \{(Y - R\tilde{N}_p)^{-1}(X + R\tilde{D}_p) | R \in M(RH^\infty), \det(Y - R\tilde{N}_p) \neq 0\} = \{(\tilde{X} + D_p Q)(\tilde{Y} - N_p Q)^{-1} | Q \in M(RH^\infty), \det(\tilde{Y} - N_p Q) \neq 0\}$, where (N_p, D_p), $(\tilde{N}_p, \tilde{D}_p)$ are any right and left coprime fractional factorization of $G(s)$ with the corresponding quadruple $(X, Y, \tilde{X}, \tilde{Y})$ and N_p, D_p, $\tilde{N}_p$, $\tilde{D}_p$, X, Y, $\tilde{X}$, $\tilde{Y} \in M(RH^\infty)$. Lemma 5 gives a parameterization of the objective function in terms of the free parameter R.

Lemma 5. (Parameterization) Let $F(s) \in \Omega(G)$, then

$$\begin{aligned} S^* W_1 S + T^* W_2 T &= (MN_p R\tilde{D}_p + MN_p X - M^{-*} W_1)^* \\ &\quad (MN_p R\tilde{D}_p + MN_p X - M^{-*} W_1) \\ &\quad + W_1(W_1 + W_2)^{-1} W_2 \end{aligned} \tag{1}$$

Lemma 6. 1) $W_1(W_1 + W_2)^{-1} W_2 = W_2(W_1 + W_2)^{-1} W_1$. 2) $W_1(W_1 + W_2)^{-1} W_2$ is para-Hermitian.

In Ref. 11, Helton mentioned the problem of solving $\min_{f\in D} \sup_\omega \Theta[\omega, f(j\omega)]$ (where Θ is a given positive-valued function and D is a feasible set). He claimed that many problems taking this form have the property that an optimum f_{opt} will make the objective function $\Theta[\omega, f_{\text{opt}}(j\omega)]$ constant in ω almost everywhere, that is, it will be frequency independent. This is the so-called self-flattening property. To simplify the mathematical sophistication and the computational burden that may be involved in the later design process, let us confine the feasible set of $F(s)$ to be a subset of $\Omega(G)$, expressed as $\Omega'(G)$, which makes the objective function self-flattening. That is, we look for an equalizing optimal solution. Therefore, our optimization problem becomes

$$(\bar{\text{P}}) \qquad \min_{F\in\Omega'(G)} \|S^* W_1 S + T^* W_2 T\|_\infty$$

The procedure for finding a nonequalizing solution is quite similar to finding the equalizing solution with some modifications.[12]

Solution Method

Optimal H^∞ Cost

The greatest lower bound of the H^∞ criterion, for all possible $F(s) \in \Omega'(G)$, can be easily determined based on an analysis similar to that of Kwakernaak,[5,6] and the result is summarized in the following theorem.

Theorem 1.[12] For any $F \in \Omega'(G)$, the corresponding pair (S,T) satisfies

$$\|S^* W_1 S + T^* W_2 T\|_\infty \geq \alpha_0^2$$

where $\alpha_0^2 = \max(a,b)$ and $a = \max\{\alpha^2 | \det[\alpha^2 I_n - W_1(W_1 + W_2)^{-1} W_2]|_{s=\infty} = 0\}$, $b = \max\{\alpha^2 | \det[\alpha^2 I_n - W_1(W_1 + W_2)^{-1} \times W_2](j\omega) = 0 \text{ for some } \omega\}$.

Let $\min_{F\in\Omega'(G)} \|S^* W_1 S + T^* W_2 T\|_\infty = \alpha_{\text{opt}}^2$, then, in general, $\alpha_{\text{opt}}^2 \geq \alpha_0^2$. The greatest lower bound α_0^2 is only related to the weighting matrices chosen and can be found from $\det[\alpha^2 I_n - W_1(W_1 + W_2)^{-1} W_2]$.

In Refs. 7 and 8, Helton presented a method for solving broadband circuit design problems, particularly gain equalization problems. We will borrow Helton's idea to find α_{opt}^2. Because his results are developed for the unit disk, it is more convenient at this point to map the right half-plane onto the unit disk via the bilinear mapping $s \to z = (s-1)/(s+1)$. Obviously, the two formulations are equivalent, and one can use such a transformation to convert one to another. From here until the end of this section, all complex functions are functions of z. $(RL^\infty)^{n\times n}$ and $(RH^\infty)^{n\times n}$ denote the set of all $n \times n$ matrices with bounded, real-rational elements having no poles on and inside $|z| = 1$, respectively.

Let $C(e^{j\theta})$, $P(e^{j\theta})$, $R(e^{j\theta}) \in (RL^\infty)^{n\times n}$ and P^2 and R are strictly positive definite. Define a disk $\Delta_C^{P,R}$ in the matrix function space $(RL^\infty)^{n\times n}$ to be the set of all $\Gamma(e^{j\theta}) \in (RL^\infty)^{n\times n}$, $\forall\theta \in [0, 2\pi]$ that satisfies $(\Gamma - C)P^2(\Gamma - C)^* \leq R$, i.e.,

$$\begin{aligned} \Delta_C^{P,R} = \{\Gamma \in (RL^\infty)^{n\times n} | &[\Gamma(e^{j\theta}) - C(e^{j\theta})]P^2(e^{j\theta})[\Gamma(e^{j\theta}) \\ &- C(e^{j\theta})]^* \leq R(e^{j\theta})\} \end{aligned}$$

Then the question is: given $\Delta_C^{P,R}$, does it contain a function in $(RH^\infty)^{n\times n}$? The question is answered by Theorem 2.

Theorem 2.[7,8] For a given $\Delta_C^{P,R}$ defined previously, there is a function $\Gamma \in (RH^\infty)^{n\times n}$ in this set if and only if the maximum eigenvalue $\lambda_{\max}$ of $(H_C[T_{P-2}]^{-1} H_C^*)x = \lambda T_R x$ is less than or equal to one.

Note that the generalized eigenvalue problem in Theorem 2 is infinite dimensional with block Hankel and Toeplitz matrices.

Suppose that $\bar{F}$ solves $(\bar{\text{P}})$ with the corresponding pair $(\bar{S}, \bar{T})$ and cost α_{opt}^2. Then

$$\bar{S}^* W_1 \bar{S} + \bar{T}^* W_2 \bar{T} = \alpha_{\text{opt}}^2 I_n \quad \text{with} \quad \alpha_{\text{opt}}^2 \geq \alpha_0^2$$

where α_0^2 is determined from Theorem 1. Let us consider the following problem:

$$S^*W_1S + T^*W_2T = (\alpha_0^2 + \epsilon)I_n \quad \text{where} \quad \epsilon \geq 0 \tag{2}$$

From Lemma 5, Eq. (2) can be written as

$$(MN_pR\tilde{D}_p + MN_pX - M^{-*}W_1)^*$$
$$(MN_pR\tilde{D}_p + MN_pX - M^{-*}W_1)$$
$$= (\alpha_0^2 + \epsilon)I_n - W_1(W_1 + W_2)^{-1}W_2 \tag{3}$$

Define

$$C = M^{-*}W_1 \in (RL^\infty)^{n\times n} \tag{4a}$$

$$\Gamma = MN_pR\tilde{D}_p + MN_pX \in (RH^\infty)^{n\times n} \tag{4b}$$

$$Q_\epsilon = (\alpha_0^2 + \epsilon)I_n - W_1(W_1 + W_2)^{-1}W_2 \in (RL^\infty)^{n\times n} \tag{4c}$$

Then Eq. (3) becomes

$$[\Gamma(e^{j\theta}) - C(e^{j\theta})]^*[\Gamma(e^{j\theta}) - C(e^{j\theta})] = Q_\epsilon(e^{j\theta}), \quad \theta \in [0,2\pi] \tag{5}$$

Note that C is determined by W_1 and W_2, and therefore it is known in advance. The para-Hermitian matrix Q_ϵ is a function of ϵ and $Q_\epsilon(e^{j\theta}) > 0$ for $\epsilon > 0$.

Letting Eq. (5) define a "disk" Δ_ϵ as

$$\Delta_\epsilon = \{\Gamma \in (RL^\infty)^{n\times n} | [\Gamma(e^{j\theta}) - C(e^{j\theta})]^*[\Gamma(e^{j\theta}) - C(e^{j\theta})]$$
$$\leq Q_\epsilon(e^{j\theta});\ \forall\theta \in [0,2\pi]\}$$

with C and Q_ϵ defined in Eqs. (4a) and (4c) and $\epsilon > 0$. Then finding α_{opt}^2 is equivalent to solving the problem (P1): min $\{\epsilon | \epsilon \geq 0,\ \Delta_\epsilon \cap (RH^\infty)^{n\times n} \neq \emptyset\}$. Therefore, solving the controller design problem is equivalent to performing the following three steps: 1) solve problem (P1); 2) if ϵ_0 solves (P1) (i.e., $\alpha_{\text{opt}}^2 = \alpha_0^2 + \epsilon_0$), then find the $\tilde{\Gamma} \in (RH^\infty)^{n\times n}$ that satisfies $(\tilde{\Gamma} - C)^*(\tilde{\Gamma} - C) = Q_{\epsilon_0}$; and 3) based on $\tilde{\Gamma}$, use Eq. (4b) to find the corresponding $\tilde{R}$.

To solve the preceding problem, consider the following analog of Theorem 2.

Theorem 3.[12] Consider problem (P1) and its corresponding generalized eigenvalue problem (P2): $(H_C^*H_C)x = \lambda T_{Q_\epsilon}x$, where C, Q_ϵ are defined in Eqs. (4a) and (4c). Then, $\Delta_\epsilon \cap (RH^\infty)^{n\times n} \neq \emptyset$ if and only if $\lambda_{\max}(\epsilon) \leq 1$, where $\lambda_{\max}(\epsilon)$ is the maximum eigenvalue of (P2).

On the unit circle, all of the eigenvalues of (P2) are real and non-negative for $\epsilon > 0$. The eigenvalue $\lambda_{\max}(\epsilon)$ is a strictly monotonically decreasing function of ϵ (Refs. 12 and 13). Using this property, it is easy to find ϵ_0 numerically using, for example, Newton's method. Note that if $\lambda_{\max}(0) \leq 1$ then $\epsilon_0 = 0$, and if $\lambda_{\max}(0) > 1$ then ϵ_0 is the minimum ϵ such that $\lambda_{\max}(\epsilon_0) = 1$.

Some Remarks About Computing $\lambda_{\max}(\epsilon)$

The problem (P2) is infinite dimensional. To compute $\lambda_{\max}(\epsilon)$ numerically one can truncate the infinite block Hankel and Toeplitz matrices in (P2) to finite ones. The reduced generalized eigenvalue problem can then be solved by existing software packages such as EISPACK, IMSL, etc. For low-pass generating functions, as is usually the case, the higher order coefficients of the power series expansion on the unit circle converge to zero very quickly. Therefore, these coefficients have less effect on their corresponding Hankel and Toeplitz matrices in problem (P2). The accuracy of this approximation depends on how fast these coefficients converge to zero.

Another way to compute $\lambda_{\max}(\epsilon)$ numerically without truncation is to convert (P2) into the equivalent problem: $(H_{CL^{-1}})^*(H_{CL^{-1}})x = \hat{\lambda}x$, where $L(\epsilon)$ is a spectral factor of Q_ϵ. By applying the properties of Hankel and Toeplitz operators,[14] the conversion can be performed easily. Then, finding $\lambda_{\max}(\epsilon)$ of (P2) is equivalent to finding the maximum singular value of $H_{CL^{-1}}$, i.e., $\lambda_{\max}(\epsilon) = \hat{\lambda}_{\max}(\epsilon) = \bar{\sigma}^2(H_{CL^{-1}})$. The stable part (i.e., $[CL^{-1}]_+$) of CL^{-1} determines the Hankel matrix $H_{CL^{-1}}$. Because the matrix $[CL^{-1}]_+$ is real rational, from Kronecker's theorem, the induced Hankel matrix $H_{CL^{-1}}$ is of finite rank and its dimension equals the McMillan degree of $[CL^{-1}]_+$. Therefore, finding $\lambda_{\max}(\epsilon)$ is equivalent to finding the Hankel norm of $[CL^{-1}]_+$ (the maximum Hankel singular value of $[CL^{-1}]_+$). It is fairly easy to compute $\lambda_{\max}(\epsilon)$, and the steps required will be given in our design algorithm.

Controller Parameter Matrix

Assume that all of the matrices involved have been bilinearly transformed back into the s domain. We know that the optimal stabilizing controller $\tilde{F}(s)$, parameterized in terms of the controller parameter matrix $\tilde{R}(s)$, satisfies

$$(MN_p\tilde{R}\tilde{D}_p + MN_pX - M^{-*}W_1)^*$$
$$(MN_p\tilde{R}\tilde{D}_p + MN_pX - M^{-*}W_1) = Q_{\text{opt}} \tag{6}$$

with

$$Q_{\text{opt}} = \alpha_{\text{opt}}^2 I_n - W_1(W_1 + W_2)^{-1}W_2 \in (RL^\infty)^{n\times n}$$

From Lemma 6 and by factorization of $Q_{\text{opt}}(s)$ into $\Sigma^*(s)\Sigma(s)$ with $\Sigma \in (RL^\infty)^{n\times n}$, Eq. (6) implies that

$$MN_p\tilde{R}\tilde{D}_p + MN_pX - M^{-*}W_1 = U\Sigma \tag{7}$$

where U is an $n \times n$ all-pass matrix. Without losing generality, we can assume $U = I_n$.

Strict properness of $G(s)$ implies $N_p(\infty) = 0$. Therefore, from Eq. (7), we have $[\Sigma]_- = -[M^{-*}W_1]_-$. The stable part of $\Sigma(s)$ can then be determined from $[\Sigma]_-$ and $Q_{\text{opt}}(s)$. Premultiply and postmultiply Eq. (7) by M^{-1} and $\tilde{D}_p^{-1}$, respectively, and then by extracting its stable part, we get

$$N_p\tilde{R} = [M^{-1}\Sigma\tilde{D}_p^{-1}]_+ + [(W_1 + W_2)^{-1}W_1\tilde{D}_p^{-1}]_+$$
$$- [N_pX\tilde{D}_p^{-1}]_+ \tag{8}$$

Define $V = [M^{-1}\Sigma\tilde{D}_p^{-1}]_+ + [(W_1 + W_2)^{-1}W_1\tilde{D}_p^{-1}]_+ - [N_pX\tilde{D}_p^{-1}]_+$. Then, solving for the controller parameter matrix $\tilde{R}(s)$ reduces to solving a matrix equation problem, i.e., given $N_p(s) \in (RH^\infty)^{n\times m}$, and $V(s) \in (RH^\infty)^{n\times n}$ and both are strictly proper, solve $N_p(s)\tilde{R}(s) = V(s)$ so that $\tilde{R}(s) \in (RH^\infty)^{m\times n}$.

The problem of solving the rational matrix equation $T_1(s)T(s) = T_2(s)$, where $T_1(s)$ and $T_2(s)$ are given proper rational matrices with compatible dimensions, frequently arises in the synthesis of linear multivariable systems. If a proper, rational matrix solution $T(s)$ of minimal McMillan degree is desired, then this problem is called the minimal design problem (MDP). If only a proper rational solution $T(s)$ is desired, then this problem is called the exact model matching problem (EMMP). Several existing methods for solving the MDP and EMMP can be found in the literature. The problem of finding a stable solution to the MDP is difficult. However, in our case, only a stable solution is desired. Therefore, solving Eq. (8) can be viewed as a stable exact model matching problem (SEMMP), which can be solved by either a transfer function matrix factorization approach[15,16] or a geometric approach.[17]

Design Algorithm

Based on the foregoing discussion, the complete solution procedure to find the controller $\tilde{F}(s)$ that solves the problem (P̃) is summarized as follows:

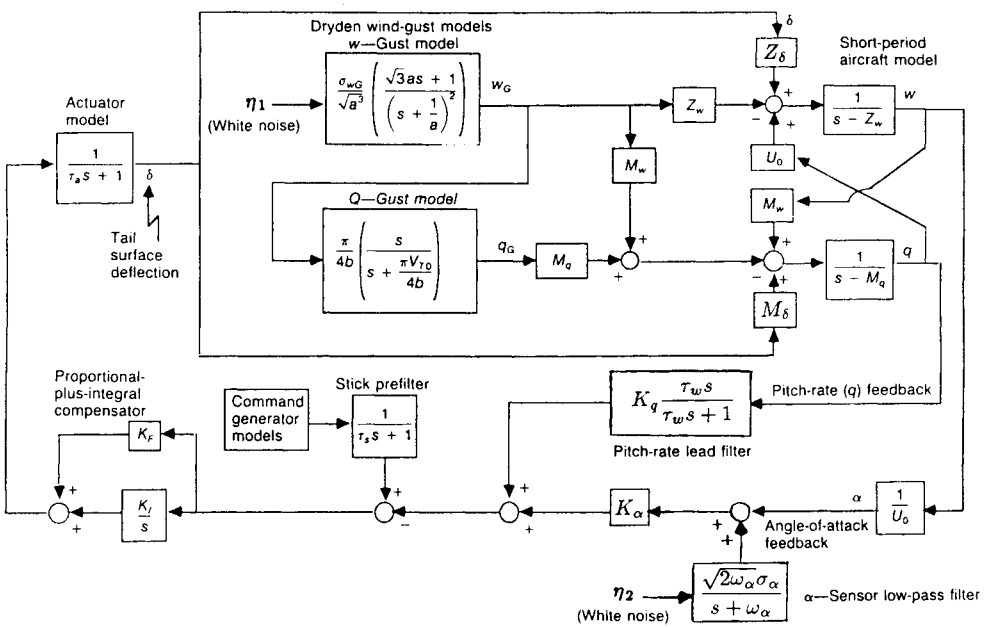

Fig. 1 Block diagram of the Grumman F-14 control problem.

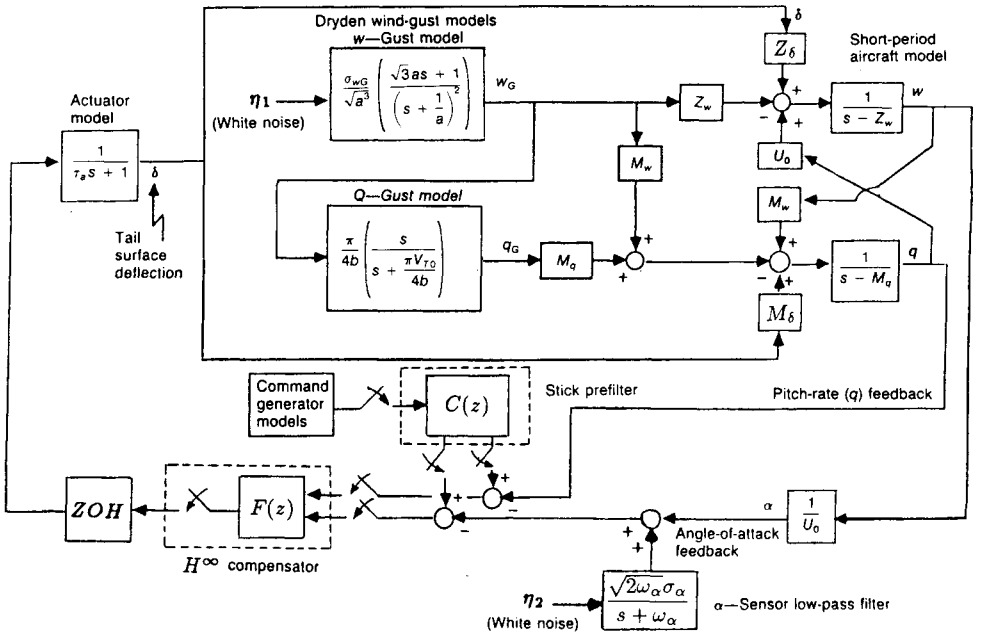

Fig. 2 Block diagram of the modified F-14 problem.

Procedure I.—Data: $\bar{W}_1$ and $\bar{W}_2$ given, set $\epsilon_0 = \epsilon$.

1) Calculate $W_1 = \bar{W}_1^* \bar{W}_1$, $W_2 = \bar{W}_2^* \bar{W}_2$, and $W_1(W_1 + W_2)^{-1}W_2$.
2) Find α_0^2 (see Theorem 1).
3) Set $C = (M^*)^{-1}W_1$.
4) Set $k = 0$.
5) Let $Q(\epsilon_k) = (\alpha_0^2 + \epsilon_k)I_n - W_1(W_1 + W_2)^{-1}W_2$.
6) Perform spectral factorization of $Q(\epsilon_k)$ so that $Q(\epsilon_k) = L_k^* L_k$.
7) Find a minimal realization (A_k, B_k, C_k) of $[CL_k^{-1}]_+$.
8) Determine the controllability and observability Gramians (P_k, Q_k) associated with (A_k, B_k, C_k).
9) Find the maximum eigenvalue $\bar{\gamma}_k$ of $P_k Q_k$.
10) If $\bar{\gamma}_0 \le 1$, set $\alpha_{\text{opt}}^2 = \alpha_0^2$, and go to procedure II.
11) If $|\bar{\gamma}_k - 1| \le \epsilon$, set $\alpha_{\text{opt}}^2 = \alpha_0^2 + \epsilon_k$, and go to procedure II.
12) Update ϵ_k ($\epsilon_{k+1} \leftarrow \epsilon_k$).
13) Set $k = k + 1$, and go to step 5.

Procedure II.—Data: $G(s)$ given.

1) Do right and left coprime factorization of $G(s)$.

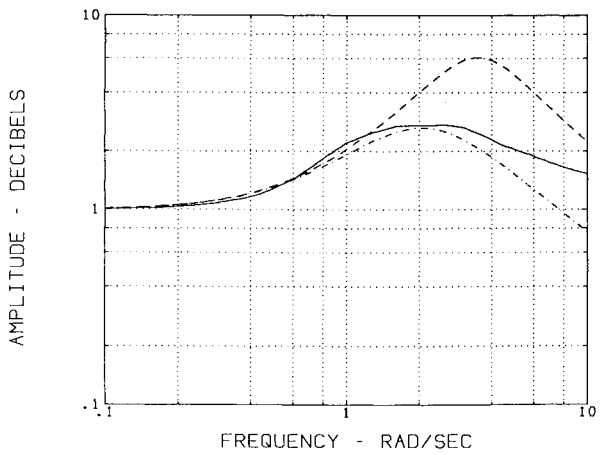

Fig. 3 Constraint bounds and normalized pitch rate amplitude response.

2) Find X and Y from known $\tilde{D}_p$, $\tilde{N}_p$, D_p, N_p.
3) Let $Q = \alpha_{\text{opt}}^2 I_n - W_1(W_1 + W_2)^{-1}W_2$.
4) Calculate $[\Sigma]_- = -[C]_-$.
5) Find $[\Sigma]_+$ from steps 3 and 4.
6) Set $\Sigma = [\Sigma]_+ + [\Sigma]_-$.
7) Form the matrix

$$V = [M^{-1}\Sigma\tilde{D}_p^{-1}]_+ + [(W_1 + W_2)^{-1}W_1\tilde{D}_p^{-1}]_+ - [N_pX\tilde{D}_p^{-1}]_+$$

8) Solve $N_p\tilde{R} = V$ so that $\tilde{R} \in R(s)^{m\times n}$ is stable and proper.
9) Form $\tilde{F} = (Y - \tilde{R}\tilde{N}_p)^{-1}(X + \tilde{R}\tilde{D}_p)$.

Stop.

Note that $\bar{\gamma}_k$ is the square of the maximum Hankel singular value of $[CL_k^{-1}]_+$ and ϵ_k can be updated by using, for example, Newton's method.

Example

Problem Descriptions

The block diagram of the Grumman F-14 pitch axis control is shown in Fig. 1[18] where the aircraft model is based on a linearization of the system about an operating point of Mach = 0.71, altitude = 35,000 ft, and total airspeed = 690.4 ft/s [$Z_\delta = -63.9979$ ft/(rad-s^2), $M_\delta = -6.8847$ (rad-s^2)$^{-1}$, $U_0 = 689.4$ ft/s, $M_w = -5.92 \times 10^{-3}$ (ft-s)$^{-1}$, $Z_w = -0.6385$ s^{-1}, $M_q = -0.6571$ s^{-1}, and $\tau_a = 0.05$ s]. The vertical velocity wind gust w_G and the pitch-rate wind gust q_G, which are generated by a white noise η_1 with a power spectrum $(2\pi)^{-1}$, are injected into the system. The α-sensor noise, generated by a white noise η_2 with a power spectrum $(2\pi)^{-1}$, also exists in the feedback loop ($a = 2.5348$ s, $b = 64.13$ ft, $V_{T0} = 690.4$ ft/s, $\sigma_{wG} = 3.0$ ft/s, $\sigma_\alpha = 5.236 \times 10^{-3}$ rad, and $w_\alpha = 10.0$ rad/s). In the original design by Grumman, the controller structure was fixed in advance and the six parameters denoted by τ_s, τ_ω, K_α, K_q, K_F, K_I were adjusted to meet the design specifications.[18]

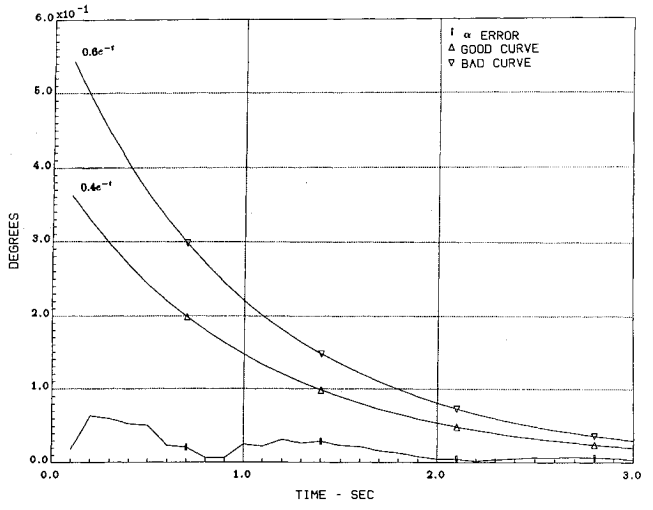

Fig. 4 Model-following error for the designed system.

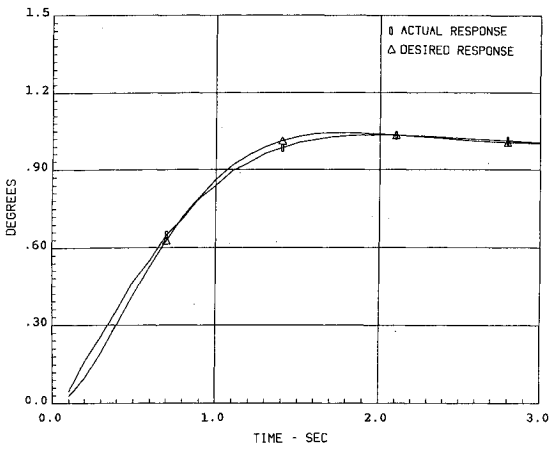

Fig. 5 Comparison of actual and desired α step responses.

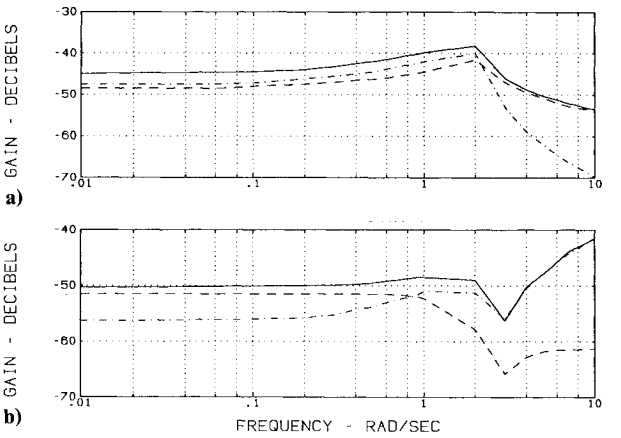

Fig. 6 Gains and σ plots of disturbances and noise on α and q.

Because the digitized controller is more realistic, given current technology, as well as a more interesting challenge due to the effects of sampling, we will design a discrete time controller even though the benchmark is in continuous time. The modified system is shown in Fig. 2. The design problem is to develop a control system such that the closed-loop response to a pilot-commanded 1-deg change in angle of attack $\alpha(t)$ approximates the response of a second-order system with damping ratio $\xi = 0.707$ and bandwidth $\omega_n = 2.49$ rad/s. The normalized gain $|q(j\omega)|_{\text{nom}}$ of the pitch-rate response to stick input for $0.1 \le \omega \le 10$ rad/s is to fall within the bounds (dashed lines) of Fig. 3. In addition, the control system is to be optimized in terms of its aerodynamic parameter variations reduction and disturbance rejection to modeled wind gust and α-sensor noise. Estimates of the likely variation in the parameters of the model were obtained. These are: $Z_\delta \pm 50$, $M_\omega \pm 25$, $M_q \pm 50$, $M_\delta \pm 25$, $\tau_a \pm 10$, and $Z_\omega \pm 20\%$.

Controller Design

The design process is divided into two separate parts. The controller $F(z)$ will be determined by the design algorithm so as to maximize the robustness of the closed-loop system. The precompensator $C(z)$ will be chosen to shape $\alpha(t)$ and $|q(j\omega)|_{\text{nom}}$ to meet the desired constraints.

Based on the plant characteristics $G(s)$ and the system bandwidth, a 20-Hz sampling rate is selected. The discrete version of the plant $G(z)$, which includes a zero-order hold and the actuator, is then found. From the given wind gust and α-sensor noise models, we estimate the main frequency ranges of the wind gust disturbances and α-sensor noise, respectively, to determine the weights. Their discrete equivalents are then obtained by performing Tustin's transformation. Finally, the weighting matrices on S and T are chosen to be $\bar{W}_1(z) = 0.1(z + 1.0)(1.1z - 0.9)^{-1}I_2$ and $\bar{W}_2(z) = (z + 1.0)(3.0z - 1.0)^{-1}I_2$. For $\bar{W}_1$, a first-order low-pass filter is used on α and q with good disturbance rejection up to about 2 rad/s. For $\bar{W}_2$, a first-order high-pass filter with a cutoff frequency of 10 rad/s is used to limit the system bandwidth for robustness.

Following the design procedures I and II, we found that $\alpha_{\text{opt}}^2 = 0.5$. The stabilizing controller $F(z)$ is a 1×2 real-rational, proper transfer matrix with gains 15.8942 and 3.5333 and poles 0.8268, 0.7959, 0.5113, 0.50, 0.3244, 0.2342, $0.5218 \pm j0.4726$, $-0.5451 \pm j0.1884$, and $0.9281 \pm j9.5398 \times 10^{-2}$. The controller zeros are at $0.9281 \pm j0.2504$, $0.9309 \pm j0.1197$, 0.7509, -0.5113, -0.50, -0.3137, 0.1306, 1.4104×10^{-2}, $-0.6010 \pm j0.1912$, and 0.9398, $0.9126 \pm j0.1614$, 0.6944, 0.4648, -0.6361, $-0.4334 \pm j0.1077$, -0.50, -0.5113, -0.3008, and 0.1347. Note

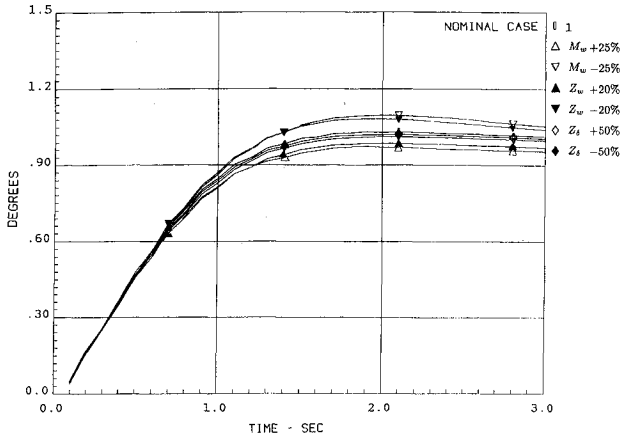

Fig. 7 The α responses under M_w ($\pm 25\%$), Z_w ($\pm 20\%$), and Z_δ ($\pm 50\%$) variations.

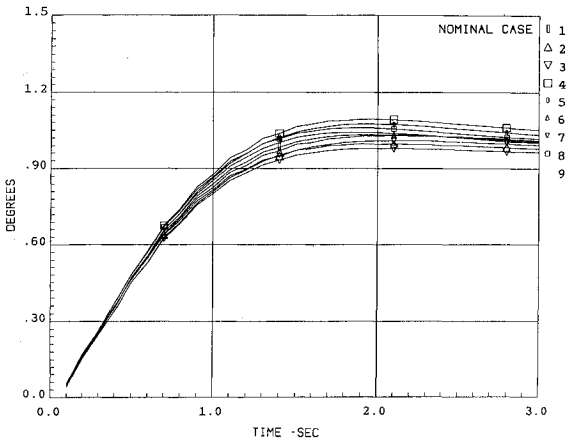

Fig. 8 Some representative α responses under parameter simultaneous variations.

that we cannot directly solve step 8 of procedure II due to the instability of $(N_p^T N_p)^{-1} N_p^T$; therefore, we used Packard and Sastry's method[16] to find $\tilde{R}(z)$. The control design using H^∞ methods often induces a high-order controller. In this example, although $F(z)$ is of order 12, the controller order can be reduced to 6 without introducing too much error.[19]

We take the simplest possible structure for $C(z)$ and assume that it has the following form:

$$C(z) = \begin{bmatrix} k_1(z+\alpha_1) & (z+\beta_1)^{-1} \\ k_2(z+\alpha_2) & (z+\beta_2)^{-1} \end{bmatrix}$$

with $|\beta_1| < 1$ and $|\beta_2| < 1$. To get a good tracking on $\alpha(t)$, we change the Grumman requirement on the α error from ≤ 0.1 to $\leq 0.4e^{-t}$ to force the model following error to go to zero as t becomes large. We then run Console,[20] an optimization-based computer-aided design (CAD) software, to find the parameters for $C(z)$ to satisfy the design constraints. Note that the robustness has nothing to do with the precompensator design, and a good matching with the constraints will not improve the robustness.

Simulations

Model-Following Error, α, and q Responses

The absolute value of the model-following error and its corresponding good and bad curves are shown in Fig. 4. From this figure, we see that the α error is small and lies far below its good curve $0.4e^{-t}$. Obviously, it satisfies the original Grumman requirement (i.e., ≤ 0.1 deg), which is less stringent than the "good" curve chosen. The maximum α error is 0.0639 deg, which occurs at $t = 0.2$ s, and the error reduces to 2.79×10^{-3} deg at $t = 3$ s. The α step response is shown in Fig. 5.

The frequency range over which the optimization was conducted was chosen to span the pilot's short-period frequency range of interest (nominally 0.1–10 rad/s). The normalized pitch-rate amplitude response over that range is shown in Fig. 3 (solid line). In the frequency range 0.66–1.05 rad/s, the gain slightly exceeds the given upper bound, and the worst point occurs at $\omega = 0.9$ rad/s where the deviation is 0.58 dB. In the frequency range 0.1–0.56 rad/s the gain is slightly less than its lower bound but no larger than 0.3 dB from it. This -0.3-dB point occurs at $\omega = 0.4$ rad/s. In the other frequency range, the pitch-rate gain lies between the given bounds. The further improvement of these soft constraints violation is possible by changing the initial values of the design parameters in $C(z)$ and resuming the optimization process.

Effects of External Disturbances on System Outputs

The effects of wind gust disturbance and α-sensor noise on the system output responses, α and q, are shown in Fig. 6. The two dashed lines in Fig. 6a represent the gains from the wind gust disturbance to q and α, respectively. We see that the disturbance has negligible effects on both α and q because within the significant frequency range of the wind gust (≤ 2 rad/s) its gain values lie between -40.0 dB ~ -60.0 dB. This approximately corresponds to 0.005–0.001-deg (deg/s) fluctuation on α (q), which, obviously, is quite small. The two dashed lines in Fig. 6b represent, respectively, the noise effects on α and q responses. The main frequency range of α-sensor noise is below 10 rad/s and its gain values within that range lie below -40.0 dB, very small compared with the corresponding α and q plots. Note that the pitch-rate gain we found is greater than -10 dB in the range 0.01–10 rad/s. The two solid lines in Fig. 6 show the maximum singular values (i.e., $\bar{\sigma}$ plot) of the wind gust disturbances (w_G, q_G) and sensor noise matrices associated with α and q responses. Obviously, they have negligible effects on the system outputs.

Robustness of α Response Under Aircraft Parameter Variations

The α response of the system by varying the parameters Z_δ, M_w, M_q, M_δ, τ_a, and Z_w by ± 50, ± 25, ± 50, ± 25, ± 10, and $\pm 20\%$, respectively, are also examined. We found that the α response is very robust against parameters Z_δ, M_q, and τ_a variations, and only very small deviations from its nominal response can be observed. However, the α response is more sensitive relative to M_w and M_δ variations. Increasing $|M_\delta|$ beyond 20% will deteriorate its response and cause oscillations. Reducing the actuator time constant $|\tau_a|$ by 10% will also introduce oscillations, but its effect is much smaller and less obvious. The α response under M_w ($\pm 25\%$), Z_w ($\pm 20\%$), and Z_δ ($\pm 50\%$) variations are shown in Fig. 7. From simulations, we found that the α response of the designed system is quite robust against each individual parameter variation, and its steady-state value lies between 0.9 and 1.1, which satisfies the original design requirement. Note that ± 0.1-deg deviation from its final value is considered good for the original Grumman specification for $\alpha(t)$.

We also performed extensive simulation study by varying the six parameters simultaneously. Among those combinations, most of them are taken under the worst case, i.e., we let each parameter change at its maximum allowance. Figure 8 shows some of the representative α responses under the six parameters, simultaneous perturbations. Nearly 65 possible combinations were examined, and we found that the α responses are still quite well-behaved and no big overshoot occurs. Some of the combinations do exhibit oscillations during the transients, but their amplitudes remain within ± 0.1 deviations as compared to the nominal α response. It is possible to further improve the system robustness by changing the weights.[21]

Conclusions

The robust controller design based on the minimization of the H^∞ norm of a mixed sensitivity function is proposed. Two weighting functions are introduced in the control design to trade off between feedback properties in different frequency

ranges. By changing the Bode plots of these two weights, we can adjust the design performance until the robustness of the designed system becomes satisfactory. The design algorithm is applied to design a robust controller for a digitized model of the F-14 aircraft. In this two-degree-of-freedom structure, the H^∞ controller is designed via our method to optimize the robustness of the system. The precompensator is used to shape the output responses so as to cause the entire system to achieve the desired performance. The effects of the external disturbances and the robustness of the angle-of-attack response under the large aircraft parameter variations are also examined.

Appendix

Proof of Lemma 3. $W_1(s)$ and $W_2(s)$ are Hermitian matrices on the $j\omega$ axis and also non-negative definite for all ω; therefore, $\det(W_1 + W_2)(j\omega) \geq \det[W_1(j\omega)] + \det[W_2(j\omega)] \neq 0$. This implies that $(W_1 + W_2)^{-1}$ exists on the $j\omega$ axis. □

Proof of Lemma 5. Let $G = N_p D_p^{-1} = \tilde{D}_p^{-1}\tilde{N}_p$ with the corresponding quadruple $(X, Y, \tilde{X}, \tilde{Y})$, i.e., $XN_p + YD_p = I_m$, $\tilde{N}_p\tilde{X} + \tilde{D}_p\tilde{Y} = I_n$. Because $T = (I_n + GF)^{-1}GF = G(I_m + FG)^{-1}F$, we have $T = N_p D_p^{-1}[I_m + (Y - R\tilde{N}_p)^{-1}(X + R\tilde{D}_p)N_p D_p^{-1}]^{-1}F = N_p D_p^{-1}\{(Y - R\tilde{N}_p)^{-1}[(Y - R\tilde{N}_p)D_p + (X + R\tilde{D}_p)N_p]D_p^{-1}\}^{-1}(Y - R\tilde{N}_p)^{-1}(X + R\tilde{D}_p) = N_p(YD_p + XN_p)^{-1}(X + R\tilde{D}_p) = N_p(X + R\tilde{D}_p)$.

Therefore, $S = I_n - N_p(X + R\tilde{D}_p)$ and

$$T^*W_2T = \tilde{D}_p^*R^*N_p^*W_2N_pR\tilde{D}_p + \tilde{D}_p^*R^*N_p^*W_2N_pX + X^*N_p^*W_2N_pR\tilde{D}_p + X^*N_p^*W_2N_pX$$

$$S^*W_1S = \tilde{D}_p^*R^*N_p^*W_1N_pR\tilde{D}_p + (\tilde{D}_p^*R^*N_p^*W_1N_pX + X^*N_p^*W_1N_pR\tilde{D}_p - \tilde{D}_p^*R^*N_p^*W_1 - W_1N_pR\tilde{D}_p) + (W_1 - X^*N_p^*W_1 - W_1N_pX + X^*N_p^*W_1N_pX)$$

After combining the preceding two expressions, we get

$$S^*W_1S + T^*W_2T = \tilde{D}_p^*R^*N_p^*(W_1 + W_2)N_pR\tilde{D}_p + \tilde{D}_p^*R^*N_p^*[(W_1 + W_2)N_pX - W_1] + [X^*N_p^*(W_1 + W_2) - W_1]N_pR\tilde{D}_p + [W_1 + X^*N_p^*(W_1 + W_2)N_pX - W_1N_pX - X^*N_p^*W_1]$$

Let M be a spectral factor of $W_1 + W_2$; then

$$S^*W_1S + T^*W_2T = (MN_pR\tilde{D}_p)^*(MN_pR\tilde{D}_p) + (MN_pR\tilde{D}_p)^*(MN_pX - M^{-*}W_1) + (MN_pX - M^{-*}W_1)^*(MN_pR\tilde{D}_p) + [X^*N_p^*(W_1 + W_2)N_pX - W_1N_pX - (W_1N_pX)^* + W_1]$$

Note that $M^{-*} = (M^{-1})^* = (M^*)^{-1}$. By completion of the square in R we have

$$S^*W_1S + T^*W_2T = (\tilde{D}_p^*R^*N_p^*M^* + X^*N_p^*M^* - W_1M^{-1})(MN_pR\tilde{D}_p + MN_pX - M^{-*}W_1) + W_1 - W_1N_pX - X^*N_p^*W_1 + X^*N_p^*M^*MN_pX - (X^*N_p^*M^* - W_1M^{-1})(MN_pX - M^{-*}W_1)$$

$$S^*W_1S + T^*W_2T = (MN_pR\tilde{D}_p + MN_pX - M^{-*}W_1)^*(MN_pR\tilde{D}_p + MN_pX - M^{-*}W_1) + W_1 - W_1(W_1 + W_2)^{-1}W_1$$

Because $W_1 - W_1(W_1 + W_2)^{-1}W_1 = W_1[I_n - (W_1 + W_2)^{-1}W_1] = W_1(W_1 + W_2)^{-1}[(W_1 + W_2) - W_1] = W_1(W_1 + W_2)^{-1}W_2$, we get the result. □

Proof of Lemma 6. From Lemma 5, we have $W_1 - W_1(W_1 + W_2)^{-1}W_1 = W_1(W_1 + W_2)^{-1}W_2$. The matrix $W_1 - W_1(W_1 + W_2)^{-1}W_1$ can also be written as $W_1 - W_1(W_1 + W_2)^{-1}W_1 = [I_n - W_1(W_1 + W_2)^{-1}]W_1 = [(W_1 + W_2) - W_1](W_1 + W_2)^{-1}W_1 = W_2(W_1 + W_2)^{-1}W_1$. We have $W_1(W_1 + W_2)^{-1}W_2 = W_2(W_1 + W_2)^{-1}W_1$.

By Lemmas 1 and 4, $[W_1(W_1 + W_2)^{-1}W_2]^* = W_2^*(M^*M)^{-*}W_1^* = W_2(M^*M)^{-1}W_1 = W_2(W_1 + W_2)^{-1}W_1 = W_1(W_1 + W_2)^{-1}W_2$. Therefore, $W_1(W_1 + W_2)^{-1}W_2$ is para-Hermitian. □

Acknowledgments

The author would like to thank the Graduate School of the University of Minnesota, Minneapolis, for supporting this work, and the anonymous reviewers for their excellent comments and suggestions to improve the paper.

References

[1]Zames, G., "Feedback and Optimal Sensitivity: Model Reference Transformations, Multiplicative Seminorms, and Approximate Inverses," *IEEE Transactions on Automatic Control,* Vol. 26, No. 2, 1981, pp. 301-320.

[2]Francis, B. A., and Doyle, J. C., "Linear Control Theory with an H^∞ Optimality Criterion," *SIAM Journal of Control and Optimization,* Vol. 25, No. 4, 1987, pp. 815-844.

[3]Francis, B. A., *A Course in H_∞ Control Theory,* Springer-Verlag, New York, 1987.

[4]Foo, Y. K., and Postlethwaite, I., "An H^∞ Minimax Approach to the Design of Robust Control Systems," *Systems and Control Letters,* Vol. 5, No. 2, 1984, pp. 81-88.

[5]Kwakernaak, H., "Minimax Frequency Domain Performance and Robustness Optimization of Linear Feedback Systems," *IEEE Transactions on Automatic Control,* Vol. 30, No. 10, 1985, pp. 994-1104.

[6]Kwakernaak, H., "A Polynomial Approach to Minimax Frequency Domain Optimization of Feedback Systems," *International Journal of Control,* Vol. 44, No. 1, 1986, pp. 117-156.

[7]Helton, J. W., "Broadbanding: Gain Equalization Directly from Data," *IEEE Transactions on Circuits and Systems,* Vol. 28, No. 12, 1981, pp. 1125-1137.

[8]Helton, J. W., "Non-Euclidean Functional Analysis and Electronics," *Bulletin of the American Mathematical Society,* Vol. 7, No. 1, 1982, pp. 1-64.

[9]Youla, D. C., "On the Factorization of Rational Matrices," *IRE Transactions on Information Theory,* July 1961, pp. 172-189.

[10]Vidyasagar, M., *Control System Synthesis—A Factorization Approach,* Massachusetts Inst. of Technology Press, Cambridge, MA, 1985.

[11]Helton, J. W., "Worst Case Analysis in the Frequency Domain: The H^∞ Approach to Control," *IEEE Transactions on Automatic Control,* Vol. 30, No. 12, 1985, pp. 1154-1170.

[12]Yang, J.-S., "An H^∞ Method for the Design of Linear Time-Invariant Multivariable Sampled-Data Control Systems," Ph.D. Thesis, Dept. of Electrical Engineering, Univ. of Maryland, College Park, MD, 1988.

[13]Chu, C. C., and Doyle, J. C., "The General Distance Problem in H^∞ Synthesis," *International Journal of Control,* Vol. 44, No. 2, 1986, pp. 565-596.

[14]Brown A., and Halmos, P. R., "Algebraic Properties of Toeplitz Operators," *Zhurnal für die Reine und Angewandte Mathematik,* Vol. 213, Dec. 1962, pp. 89-102.

[15]Wolovich, W. A., Antsaklis, P., and Elliot, H., "On the Stability of Solutions to Minimal and Nonminimal Design Problems," *IEEE Transactions on Automatic Control,* Vol. 22, No. 1, 1977, pp. 88-94.

[16]Packard, A. K., and Sastry, S. S., "Solving Rational Matrix Equations in the State Space with Applications to Computer-Aided Control System Design," *International Journal of Control,* Vol. 43, No. 1, 1986, pp. 65-90.

[17]Hautus, M. J., "(A,B) Invariant and Stabilizability Subspaces: A Frequency Domain Description," *Automatica,* Vol. 16, No. 4, 1980, pp. 703-707.

[18]"User Data Package for Interim Cascade Program: CSCDE0.1," Grumman Aerospace Corp., EG-FC-83-39, Oct. 1983.

[19]Yang, J.-S., "On Output Frequency-Weighted Controller Reduction," *Proceedings of the 30th IEEE Conference on Decision and Control,* Vol. 1, IEEE, Piscataway, NJ, 1991, pp. 245-247.

[20]Fan, M. K. H., Tits, A. L., Zhou, J., Wang, L. S., and Koninckx, J., "CONSOLE User's Manual," System Research Center, Univ. of Maryland, College Park, MD, 1990.

[21]Yang, J.-S., "Robustness Improvement of the Grumman F-14 Benchmark Control Problem Using H^∞ Optimization," *Proceedings of the Third International Conference on Control,* Vol. 1, IEE, London, England, UK, 1991, pp. 196-201.